Formation, structure, and dissociation dynamics of CO_2^{q+} ($q \leqslant 3$) ions due to impact of 12-keV electrons

Pragya Bhatt, Raj Singh, Namita Yadav, and R. Shanker*
Atomic Physics Laboratory, Department of Physics, Banaras Hindu University, Varanasi 221005, India
(Received 13 January 2012; published 6 April 2012)

The electron-impact multiple ionization and subsequent dissociation of CO_2 is studied for 12-keV electron energy using a linear time-of-flight mass spectrometer coupled with a multihit, position-sensitive detector. The complete as well as incomplete Coulomb explosion pathways for CO_2^{2+} and CO_2^{3+} ions are examined and identified. The kinetic energy release distributions for these precursor ions are obtained. The experimental kinetic energy release values for the complete Coulomb fragmentation channels are found to be overestimated by those calculated from the Coulomb explosion model. From the angular correlation studies, it is inferred that bent geometrical states are involved for most of the fragmentation channels of CO_2^{2+} and CO_2^{3+} ions. The concerted and/or sequential nature of all the dissociation pathways is also assigned. This study provides the first results on energetics associated with the charge separation in dissociative ionization of CO_2 under the impact of electrons at a subrelativistic energy.

DOI: 10.1103/PhysRevA.85.042707 PACS number(s): 34.80.Gs, 34.80.Ht

I. INTRODUCTION

The processes of dissociation of multiply ionized molecules have been studied extensively in the past [1,2] and references therein. The understanding of such processes is important in wide areas of physical sciences, ranging from planetary and interstellar space [2] to radiation damage of biological tissues [3]. In the complete Coulombic explosion (CE) of molecular ions, if all the fragment ions are detected in coincidence, they are able to provide kinematically complete information about the molecular breakup process [1,4]. In such processes, kinetic energy release (KER), given by the sum of kinetic energies (KEs) of the individual fragments, and angular correlations of different fragment ions are of central interest in determining the structural properties of the precursor molecular ion. Studies on polyatomic molecules have shown that the interaction with energetic radiations creates noticeable changes in the molecular geometry [5–7]. The energy deposited in the molecular system by these ionizing radiations is converted into the KEs of individual fragments plus the excitation energy of the molecular species which is emitted in the form of photons [8].

In earlier experiments, time-of-flight (TOF) spectrometers [9] were employed which helped in resolving the momentum components of dissociating ions only along the axis of the spectrometer. These experiments provided easy identification of the mass-to-charge ratios of the detected ions and calculation of their ionization cross sections and the KER in a given dissociation channel. A pioneer work in this field was done by applying the idea of covariance of singles TOF spectra of ions to generate double- and triple-ion coincidence maps to predict the dissociation dynamics of various channels involved in these maps [10–12]. This technique was not able to provide the total momentum of the fragmenting ions. The advent of position-sensitive detectors (PSDs) coupled with TOF spectrometers worked as the probe to provide various unprecedented results [1,13,14]. With the help of this probe, the total momentum vectors of each ionic fragment produced in a given dissociation channel can be measured and correlated to get information about all kinematic parameters of that channel. A further breakthrough in this field was achieved when energy-selected electrons were used to tag the states of the dicationic precursor to study the selected fragmentation pathways [15,16].

The CO_2 molecule has received large attention in the past owing to its importance in our planetary atmosphere and interstellar space and is considered a key factor in determining the global warming effect [17,18]. There are numerous studies reported in the literature for electron, ion, intense laser beam, and synchrotron radiation induced dissociation of CO_2 [5,6,8,19–32]. Various mechanisms have been suggested for the dissociation of CO_2^{2+} and CO_2^{3+} precursor ions, depending upon the energy and the source of excitation/ionization [5,6,8,19–22,25,29–32]. However, the electron-impact ionization of CO_2 and its subsequent dissociation mechanisms under subrelativistic impact energies are scarce in the available literature. Furthermore, the theoretical calculations for potential energy surfaces involved in the dissociation of an individual precursor ion of multiply ionized CO_2 are also scarce owing to the large number of contributing states having very complex structures [33–35].

Under high-energy charged particle impact, the molecules have no time to rotate during the collision process and the KER in the process directly reflects the properties of excited states of the parent precursor ion. Usually, a simple picture of CE is assumed to describe such energy distributions. It is assumed here that the charges on fragment ions are pointlike and the equilibrium distance between them is used to calculate the Coulomb potential energy, which is equivalent to the sum of KEs of the fragment ions. This model is reasonably successful in predicting the most probable KER in the fragmentation of molecules of a higher degree of ionization, but for a lower degree of ionization, this model is unable to reproduce the peak values of KER distributions [22,36–38]. We have compared our experimentally observed KER values for the complete Coulomb fragmentation of CO_2^{2+} and CO_2^{3+} with those of

*shankerorama@gmail.com

the CE model to test its validity in the subrelativistic electron collisions with CO_2.

In the present work, we have used the multiple-ion coincidence technique to study the dynamics of fragment ions produced from 12-keV electron collisions with a CO_2 molecule. By measuring the total momentum vectors of the fragment ions in coincidence, the KER in different dissociation channels is obtained. The momentum and angular correlations of these fragments in various dissociation channels of ${CO_2}^{q+}$ ($q \leqslant 3$) are also obtained. With the help of shapes and slopes of the islands observed in the ion-ion coincidence map and the kinetic energies of the involved fragments, we have proposed the concerted or sequential mechanisms of fragmentation of ${CO_2}^{q+}$ ($q \leqslant 3$).

II. EXPERIMENTAL PROCEDURE

A detailed description of the experimental setup can be found in our previous papers [39,40]. Briefly, a monoenergetic beam of 12-keV electrons was extracted from a commercial electron gun. The beam was made to collide with a dilute gaseous jet of CO_2 molecules effusing from a grounded hypodermic needle (0.01 cm inner diameter and length 1.2 cm) in a cross-beam geometry. A single-stage linear TOF spectrometer [9] is used in the present experiment; the positively charged fragment ions from the collision events are extracted by application of a homogeneous electric field of 185 V/cm toward a time- and position-sensitive detector comprised of a dual-microchannel plate (MCP) with $\phi = 40$ mm and a delay line anode [41]. The ejected electrons are extracted toward a channeltron placed opposite to the direction of ion extraction. The ejected neutral particles, if any, are not detected in the present setup. The electron signal serves as the timing reference for arrival of the ions at MCP and thus provides their TOFs, while the signals from the delay line anode provide the position information of the ions on the detector. Thus, for each ion detected in coincidence, we record the TOF (t) that the ion takes from its birthplace to reach the detector and the position (x,y) where the ion has hit the detector [see Fig. 1(a)]. The employed ion detector is capable of recording the (x,y,t) information of up to four concomitant ions hitting the detector. This data is stored event by event in a list-mode file of the data acquisition module of the PC, which is used later on for offline analysis and stripping of the data. The (x,y,t) values of all ions are then converted into the corresponding momentum triplets (p_x,p_y,p_z) [39]. Once the momenta of ions are known, the dynamical properties of the ionized molecular system can be easily extracted and quantified.

III. DATA ANALYSIS AND PARAMETERS OF INTEREST

Events involving the arrival of one, two and three ions at the detector following the start pulse from an ejected electron originating from the same collision event are termed as single-, double-, and triple-ion coincidences, respectively. The raw data of single- and double-ion coincidences of CO_2 under the impact of 12-keV electrons are shown in Figs. 1(b) and 1(c)–1(d), respectively. Figure 1(b) also shows the x position of impact for each ion at the MCP together with its TOF. In practice, the ion detector detects predominantly the ions that are generated within a small collision volume and to a much lesser extent the ions that are produced along the entire path of the incident electron beam passing through the spectrometer. The presence of a large number of CO_2 and residual gas molecules in the collision zone causes a number of ions ejected from uncorrelated ionizing events also to get registered by the ion detector. Thus, in the multiple-ion coincidences, in addition to the ions generated from the same (correlated) ionization event—termed "true coincidences"—there are contributions of ions generated from different (uncorrelated) ionization events—termed "random coincidences"; the former varies linearly, whereas the latter varies quadratically with the incident beam current and the gas density. Therefore, to reduce the number of random coincidences, we have used in our experiments the lowest possible values of the incident beam current ($\leqslant$10 pA) and the gas density ($<10^{13}$ cm^{-3}).

A. Data analysis

The COBOLDPC software is used for the acquisition and offline analysis of the data. To analyze double-ion coincidences, we constrain the TOFs of the two coincident ions (t_1 and t_2) to lie in a certain range by looking at their TOF spectra. The suffixes 1 and 2 indicate the order of ion arrival at the MCP; the corresponding position (x,y) spectra for the two ions are also extracted. By knowing the two position coordinates, we can construct momenta of these ions in two directions (p_x and p_y) [39]. Momentum in the third direction (p_z) is calculated using simple equations from classical mechanics by the knowledge of an ion's TOF, the applied extraction field strength and the length parameters of the linear TOF spectrometer used in the study [39]. For triple-ion coincidences, we fix the arrival of the first ion (t_1, say for C^+) in a specific range and then sort the coincidences of second (t_2, for O^+) and third (t_3, for O^+) ion arrival following the first ion C^+; position spectra of these three ions are also extracted. The momentum triplets for these ions are calculated in a similar way as described above. Knowing the momentum components of individual ions along the three coordinate axes, the total momentum of fragment ions and hence their KEs can be easily calculated.

The raw data of double-ion coincidences shown in Figs. 1(c) and 1(d) contain true as well as random coincidences; random coincidences appear in the form of vertical or horizontal islands due to disobeying the law of conservation of momentum. During the data analysis, each event is sorted by considering both the TOF and the position information of each ion produced in that event, i.e., only those events are considered in which all six signals derived from the employed detector system (one from channeltron, one from MCP, and four signals from the delay line anode) are recorded; the details of electronic signal processing are given in Ref. [39]. This procedure improves the quality of the coincidence spectrum obtained after the offline analysis of individual dissociation channels. We have further minimized the random coincidences during the data analysis by using the momentum conservation of ions detected in coincidence. The momenta of individual ions coming from the same ionizing event should sum up

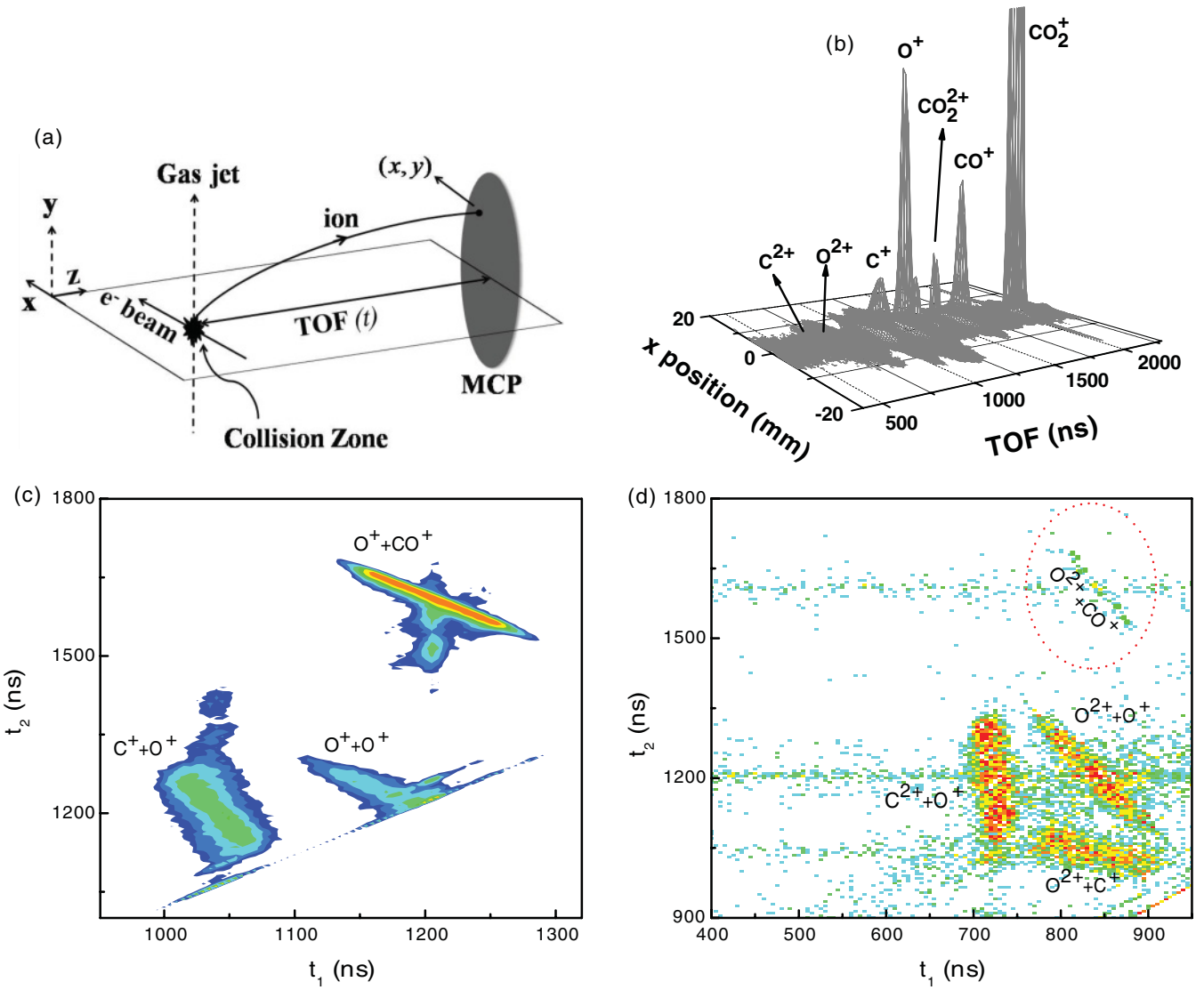

FIG. 1. (Color online) (a) Schematic diagram depicting the principle of TOF and position measurement of an ion. (b) TOF spectrum (raw data) of the produced ions along with their x positions at MCP for 12-keV electron impact with CO_2. (c) Double-ion coincidence map (raw data) observed in 12-keV electron collisions with CO_2; ion pairs result from dissociative ionization of CO_2^{2+}. (d) Same as in Fig. 1(c) but for CO_2^{3+}.

to the momentum of center of mass (CM) p_{CM} of their precursor molecular ion which is ideally zero. In practice, p_{CM} involves a finite nonzero width due to the limited temporal resolution of the system, imperfect field uniformity, and thermal motions of the molecules before ionization [11]. Thus, for the complete Coulomb fragmentation processes (involving only ions and no neutrals), we consider only those events which fall under the narrow width p_{CM} of the system, but in cases where one or more undetected neutral fragments are involved, the reported results involve comparatively higher errors because of lack of information about the undetected neutral atom or atoms. As a matter of fact, the conservation of p_{CM} is used to obtain the momentum and hence the KEs of neutral fragments for the case of incomplete Coulomb fragmentation. Furthermore, in the offline analysis, the double (or triple) ion coincidences are extracted under the condition that only two (or three) ions should be present after the prompt electron pulse. This condition further reduces the random coincidences and enables us to differentiate between two- and three-ion coincidence processes like $C^+ + O^+ + O$ and $C^+ + O^+ + O^+$.

B. Kinetic energy release distributions

The KER for a given dissociation channel is obtained by summing the KEs of individual fragments produced in that channel as follows:

$$\mathrm{KER} = \sum_i \mathrm{KE}_i = \sum_i \frac{p_i^2}{2m_i}, \tag{1}$$

where, p_i, m_i, and KE_i are the momentum, mass, and kinetic energy of ith ($i \leqslant 3$) fragment, respectively.

C. The angular and momentum correlation of fragments of a precursor ion

For obtaining angular correlations of the fragments produced in a collision event, the free angle α between their momentum vectors $\mathbf{p}_1$ and $\mathbf{p}_2$ is obtained using the relation

$$\alpha = \cos^{-1}\left(\frac{\mathbf{p}_1 \cdot \mathbf{p}_2}{p_1 p_2}\right). \tag{2}$$

The error involved in the measurement of angle α for the fragment ions of CO_2^{2+} and CO_2^{3+} is $\leqslant 10^\circ$.

To obtain the Newton diagrams, the momentum vector of the ion arriving first at MCP is taken as reference and the momentum distribution of its concomitant fragments (second ion and third ion/neutral) are plotted with respect to it.

D. Identifying the mechanisms of dissociation of a precursor ion

To extract information about the dissociation mechanisms of an ionized precursor molecule, we have made use of a method devised by Eland [11,42] which utilizes the knowledge of shapes and slopes of the islands observed in a double-ion coincidence map [see Figs. 1(c) and 1(d)]. The slope of an island can be defined as

$$\tan\theta = \frac{q_1}{q_2}\frac{p_{z2}}{p_{z1}}, \tag{3}$$

where θ is the angle subtended by the major axis of an island with the t_1 axis; q_1 and q_2 are the charge states, and p_{z1} and p_{z2} are the z components of the momentum vectors of the two fragment ions [see Fig. 1(a)].

The slopes of the islands are calculated by manual fittings on the major axis of the islands neglecting their finite widths. The shape of an island is in fact a momentum contour originating due to the momentum components of fragment ions along the spectrometer axis. A detailed description of several mechanisms suggested for the dissociation of multiply ionized molecular ions based on these shapes and slopes can be found in Refs. [11,42]. Briefly, a dissociation process is termed as concerted (c) if all the bonds of a molecule break simultaneously; it is called sequential (s) if one bond is broken and then the other one breaks eventually after a rotation of the residual CM at large distances where the Coulomb field of first fragment is negligible [8,11,42,43]. Sequential decay is further categorized into initial charge separation s(i) and deferred charge separation s(d). For the s(i) process, the slope of an island is $-(q_1/q_2)\{(m_1+m_3)/m_1\}$ or $-(q_1/q_2)\{m_2/(m_2+m_3)\}$, depending upon whether the secondary process produces the lighter ion or the heavier ion; q_1 and q_2 are the charges on masses m_1 and m_2 of the first and second fragment ions, respectively, m_3 being the mass of neutral atom produced in a given dissociation channel. However, in the s(d) process the slope is $-q_1/q_2$.

IV. RESULTS AND DISCUSSION

A. Complete Coulomb fragmentation of CO_2^{2+} and CO_2^{3+}

The Newton diagram for the $O^+ + CO^+$ channel arising from the complete Coulomb fragmentation of CO_2^{2+} is presented in the left panel of Fig. 2(a); the associated average angle between the departing fragment ions, obtained using

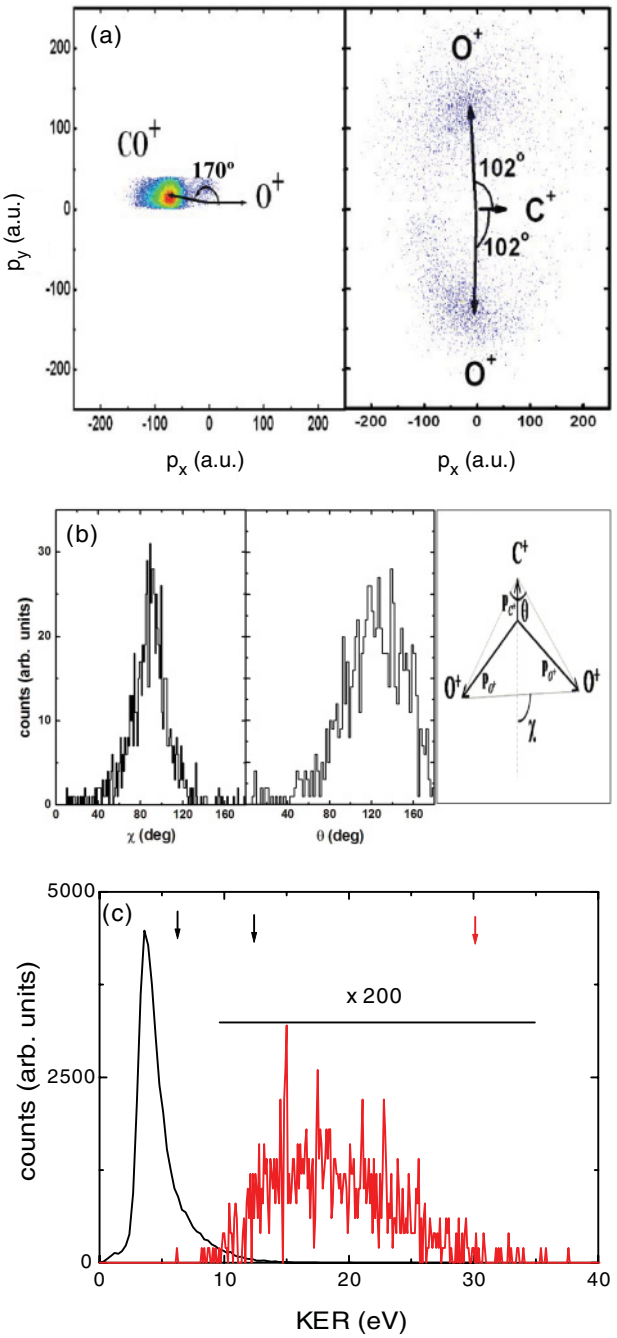

FIG. 2. (Color online) (a) Newton diagrams for complete Coulomb fragmentation channels $O^+ + CO^+$ (left) and $C^+ + O^+ + O^+$ (right) originating from the dissociation of CO_2^{2+} and CO_2^{3+}, respectively, in 12-keV electron impact with CO_2. The momentum vector of the reference ion (underlined) is taken along the x axis and the relative momentum vectors of the other ions are plotted in the upper and lower half. The average angle α between the departing fragments is also shown. (b) The distribution of angle χ (left) and the distribution of the O-C-O bond angle θ (middle) as observed in the $C^+ + O^+ + O^+$ fragmentation channel of CO_2^{3+} for 12-keV electron impact with CO_2. Definitions of angles θ and χ in momentum space (right). (c) KER distributions for the complete Coulomb fragmentation channels observed in the dissociation of CO_2^{2+} and CO_2^{3+} in 12-keV electron impact with CO_2. Black line, $O^+ + CO^+$; red line, $C^+ + O^+ + O^+$. The corresponding vertical arrows are the KER predicted by the Coulomb explosion model.

Eq. (2), is also shown. In this two-body dissociation process, momentum vectors of most of the CO^+ ions are distributed at around $170^\circ \pm 10^\circ$ with respect to the momentum vectors of O^+ ions plotted along the x axis. Similar results are reported earlier in the literature [6]. The Newton diagram for the $C^+ + O^+ + O^+$ channel is shown in the right panel of Fig. 2(a), which shows that both the O^+ ions are ejected at about 102° with respect to the momentum vector of the C^+ ion plotted along the x axis. This diagram indicates the alteration of molecular geometry for the triply ionized state of a CO_2 molecule. In fact, the theoretical calculations of the O-C-O bond angle for a CO_2 molecule at room temperature, considering its four vibrational modes, showed that the CO_2 molecule is not perfectly linear even in its ground state, its bond angle has an angular distribution from 150° to 180° centered around 172.5°, and its ionized states will be even more departed from linearity [5]. To verify this, we have measured the O-C-O bond angle θ of the dissociating precursor ion $CO_2{}^{3+}$, which is defined as the angle between the momentum vectors $\mathbf{p}_{C^+O^+}$ and $\mathbf{p}_{C^+O^+}$ as shown in the rightmost panel of Fig. 2(b). The distribution of θ is presented in the middle panel of Fig. 2(b); its mean value is estimated to be about 120°. The broad distribution of θ indicates that there are a large number of excited states involved with various bent geometries of $CO_2{}^{3+}$ precursor ions which are populated in such high-energy electron collisions with CO_2. Similar results about the bent configuration of ionized states of CO_2 are reported earlier by various workers [5,26].

To understand the dissociation mechanisms of a $CO_2{}^{2+}$ ion, we make use of the shape and slope of $O^+ + CO^+$ island shown in Fig. 1(c). It is to be noted here that the shapes of islands appearing in Figs. 1(c) and 1(d) are shown with raw data; however, the actual shapes are obtained after proper subtraction of false coincidences as discussed in Sec. III. The $O^+ + CO^+$ island is relatively narrow and intense in comparison to other islands observed in Figs. 1(c) and 1(d), and its slope is -1.00 ± 0.02 without accounting for the finite width of the island [see Eq. (3) and Table I], showing the fulfillment of conservation of momentum in the simple two-body fragmentation process. Similarly, the $O^{2+} + CO^+$ island [shown inside a red circle in Fig. 1(d)] arises from the complete Coulomb fragmentation of $CO_2{}^{3+}$ ion and makes a slope of -2.05 ± 0.04. Here also a simple two-body dissociation process is responsible for the formation of the $O^{2+} + CO^+$ channel. The same methodology cannot be applied for three-body dissociation of $CO_2{}^{3+}$, rather, an angle χ as defined in the rightmost panel of Fig. 2(b) was suggested [4,5,44] to find the dissociation mechanisms of highly ionized precursor ions. For the case of dissociation channel $C^+ + O^+ + O^+$ of $CO_2{}^{3+}$, we find that the distribution of χ shows a strong angular correlation and is peaked around a value of 90° [see Fig. 2(b)]—a signature that the two C-O bonds break simultaneously with the O^+ ions emitted back to back, leaving the central C^+ ion at rest. This result is verified by noting the equal values of momentum associated with the two O^+ ions in the present measurements, which is also reflected by the results of KEs of the O^+ ions, whereas the KE distribution of C^+ ions has a maximum very close to zero. This finding is in close agreement with the results of 120 keV Ar^{8+}, 5.9 MeV/u Xe^{43+}, and 5.9 MeV/u Xe^{18+} ion impact with a CO_2 molecule [5,22]. We have not observed any other dissociation mechanism except simultaneous (or concerted) breakup for $CO_2{}^{3+}$ into the $C^+ + O^+ + O^+$ channel. However, the possibility of other dissociation mechanisms may not be completely ruled out due to two reasons: (i) the energy resolution of our system is not very high, and (ii) our data has low ion-counting statistics for the triple-ion coincidences. Recently, Neumann *et al.* [8] have reported their results for the dissociation of $CO_2{}^{3+}$ for 3.2 keV/u Ar^{8+} ion impact on CO_2. They have observed two additional dissociation mechanisms besides the dominant concerted breakup as sequential decay and asynchronous decay. They were able to separate these three dissociation mechanisms of $CO_2{}^{3+}$ ion purely on the basis of their experimental data due to the higher resolution of the employed setup as compared to the previous measurements [22,26], as well as to the present work.

The KER distributions for the dissociation of $CO_2{}^{2+}$ into $O^+ + CO^+$ channel and for the dissociation of $CO_2{}^{3+}$ into $C^+ + O^+ + O^+$ channel are shown in Fig. 2(c); the mean KERs for these channels are estimated to be 4.7 ± 0.4 and 19.0 ± 0.4 eV, respectively; the KER distribution for the latter channel is relatively broader than the former. These observations may be understood by considering the complexity involved in such highly energetic electron collisions with a CO_2 molecule. Keeping in mind that the bond lengths between the atoms of neutral molecules do not remain fixed due to their thermal vibrations and stretching a bond is much easier than compressing it, thus the bond length will usually increase when some extra energy is supplied to the molecule. Such results are reported in the literature for various molecules in their ionized states [7]. The variations in the bond lengths cause the broadening of the KER distributions of the precursor molecular ion. The possible cause of long tails in KER distributions [see Fig. 2(c)] is the dissociation of one state via another due to curve crossing, which would lead to a large number of KER values. The most simple idea to understand such processes is the pure CE model. It is assumed here that the initial potential energy of the molecular ion is converted into the KEs of the fragments, the energy released is given by $q_1 q_2 / R_e$, where q_1 and q_2 are the charges on the fragment ions and R_e is the equilibrium ground-state internuclear distance of the parent molecule. Under this model, considering R_e between O and C atoms for CO_2 to be 1.16 Å [45], two KER values (6.2 and 12.4 eV) are possible for fragmentation of $CO_2{}^{2+}$ into the $O^+ + CO^+$ channel as the point charge on the CO^+ complex can be assumed to stay either near the C atom or near the O atom. This model predicts a single value of KER (30.0 eV) for the $C^+ + O^+ + O^+$ channel originating from $CO_2{}^{3+}$ [see Fig. 2(c)]. These values overestimate our corresponding experimental values of the KER. This discrepancy may arise due to the oversimplified assumption of localized point charges on the atoms. The effect of overlapping electron clouds must be considered to account for the KER of such complex precursor molecular ionic states. Discrepancy of this model with other charge-particle impact data is reported earlier in the literature; this model, however, corresponds well with the experimental data for ion impact with molecules when the degree of ionization of the molecule is high [5,38] as this situation favors the prediction of point charges to become feasible. Thus,

the point-charge assumption in the CE model for estimating the KER is not justified for low degrees of ionization of the dissociating molecule, as in the case of the present experiment. The probable electronic states of CO_2^{2+} giving rise to an $O^+ + CO^+$ channel with KER of 4.7 eV can be $^3\sum_u^-$ and $^3\prod_u$, as predicted theoretically by Hogreve [34]. No such prediction is available in the literature for the electronic states of CO_2^{3+} giving rise to the $C^+ + O^+ + O^+$ channel owing to the involvement of a large number of complex structured states of this precursor ion.

B. Incomplete Coulomb fragmentation of CO_2^{2+} and CO_2^{3+}

The Newton diagrams for the fragments produced in the incomplete Coulomb fragmentation of CO_2^{2+} are shown in Fig. 3(a); the associated average angles between the departing fragments are also shown. For the $C^+ + O^+ + O$ channel, the observed angular distribution is shown in the left panel of Fig. 3(a), which shows that the O^+ ion and the neutral O atom are ejected on average around 120° and 86° with respect to the C^+ ion, respectively. However, the angular distributions of both of the fragments are found to be doubly peaked: for O^+ at 110° and 158° and for O at 41° and 102°. Though these peaks are not resolved, even then it can be qualitatively inferred that both sequential and concerted pathways exist for this channel. In the first case, the neutral O is emitted toward C^+ at 41°, while the O^+ ion being emitted at 158° balances the momentum of the residual CM of $(C^+ + O)$ fragments pertaining to the sequential decay mechanism. However, for the concerted process, both the oxygen fragments O and O^+ are emitted away from C^+ at 102° and 110°, respectively. For the $O^+ + O^+ + C$ channel shown in the right panel of Fig. 3(a), we have found two distinct angular distributions arising from two bent dissociative states of CO_2^{2+}. This is also reflected by the presence of dual-peak distributions for the momenta leading to the corresponding features in the KEs of these fragment ions as described at the end of this section. However, only the dominant distribution is indicated in the angular distribution shown in Fig. 3(a) for the $O^+ + O^+ + C$ channel. Similar results are reported by Bapat and Sharma [6] for 1.3-keV electron impact on CO_2. The Newton diagram for fragments of the coincidence channel $O^{2+} + C^+ + O$ originating from the dissociation of a CO_2^{3+} ion is shown in Fig. 3(b). The O^{2+} ion is found to balance the momenta of residual CM of the $(C^+ + O)$ fragments; the neutral O atom is emitted toward the C^+ ion pertaining to the sequential fragmentation, as is also clear from the shape of the island for this channel discussed in the next paragraph. Newton diagrams for the other two channels arising from the dissociation of CO_2^{3+}, i.e., $C^{2+} + O^+ + O$ and $O^{2+} + O^+ + C$, are not obtained owing to their low counting statistics; a quantitative description of angular distributions in these cases is difficult to obtain. However, it can be qualitatively inferred that two distinct bent geometrical states are involved for the $O^{2+} + O^+ + C$ channel. To the best of our knowledge, no other data is available in the literature for the incomplete Coulomb fragmentation of a CO_2^{3+} ion to compare with the present results.

The mechanisms of dissociation of CO_2^{2+} and CO_2^{3+} into channels involving a neutral fragment are not so

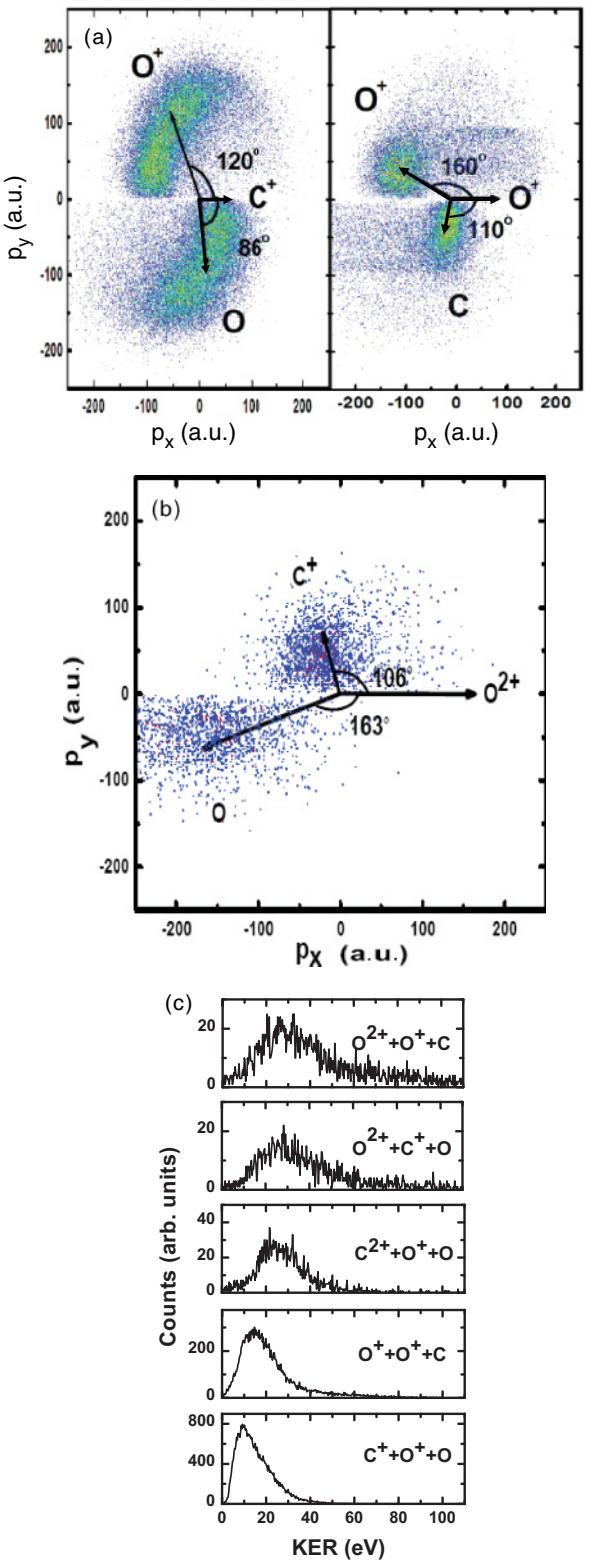

FIG. 3. (Color online) (a) The same as in Fig. 2(a) but for the incomplete Coulomb fragmentation channels $C^+ + O^+ + O$ (left) and $O^+ + O^+ + C$ (right) originating from the dissociation of CO_2^{2+}. (b) The same as in Fig. 2(a) but for the incomplete Coulomb fragmentation channel $O^{2+} + C^+ + O$ originating from the dissociation of CO_2^{3+}. (c) KER distributions for the incomplete Coulomb fragmentation channels observed in the dissociation of CO_2^{2+} and CO_2^{3+} in 12-keV electron impact with CO_2.

TABLE I. Comparison of the slopes of various islands observed in double-ion coincidence map obtained for 12-keV electron impact with CO_2 with the earlier reported experimental results and the theoretical predictions of Eland [11,42]; s(i) and s(d) refer to sequential decays with initial charge separation and deferred charge separation, respectively.

	Slope				
			Experimental results		
	Theoretical predictions		Electron impact		Photon impact
Coincidence channel	s(i)	s(d)	Present	0.6 keV[a]	0.2 keV[b]
$O^+ + CO^+$	–	–	-1.00 ± 0.02	-1.00 ± 0.02	–
$C^+ + O^+ + O$	−2.30	−1.0	-2.75 ± 0.04	-2.75 ± 0.04	–
$O^+ + O^+ + C$	−0.60	−1.0	-1.00 ± 0.02	-1.00 ± 0.04	–
$C^{2+} + O^+ + O$	−4.70	−2.0	-14.30 ± 0.05	-19.10 ± 0.02	-14.50 ± 1.50
$O^{2+} + C^+ + O$	−0.86	−2.0	-0.60 ± 0.10	-0.66 ± 0.03	-0.62 ± 0.04
$O^{2+} + O^+ + C$	−1.14	−2.0	-1.80 ± 0.14	-1.84 ± 0.03	-1.44 ± 0.04
$O^{2+} + CO^+$	–	–	-2.05 ± 0.04	-2.05 ± 0.04	–

[a]Reference [21].
[b]Reference [27].

straightforward to predict because of lack of information about the undetected neutral fragment. Therefore, we further make use of shapes and slopes of the islands in Figs. 1(c) and 1(d) to find whether the molecular ion explodes in concerted or in sequential manner. For the $C^+ + O^+ + O$ channel [see Fig. 1(c): $C^+ + O^+$ island], the slope of the island is -2.75 ± 0.04, which is in reasonable agreement with the theoretical slope of -2.30 predicted for the sequential decay [s(i)] process. However, a slight departure from the theoretical value may be attributed to the presence of the concerted process as discussed above. By studying the dissociation of CO_2 for electron energies from threshold to 600 eV, Tian and Vidal [21] had suggested that the $C^+ + O^+ + O$ channel originates purely from secondary decay for energies $\leqslant$100 eV, whereas at higher energies of impact concerted decay of the parent $CO_2{}^{2+}$ ion may also contribute to a smaller extent owing to the involvement of higher electronic states. For the $O^+ + O^+ + C$ channel of $CO_2{}^{2+}$ [see Fig. 1(c): $O^+ + O^+$ island], the slope of the island is -1.0 ± 0.02 following the concerted fragmentation. Three channels are found to originate from the incomplete Coulomb fragmentation of $CO_2{}^{3+}$, viz. $C^{2+} + O^+ + O$, $O^{2+} + C^+ + O$, and $O^{2+} + O^+ + C$ [see Fig. 1(d)]. The counting statistics for these channels are relatively low, yet the slopes of the islands can be estimated with a reasonable accuracy. The values of their slopes are found to be -14.30 ± 0.05, -0.60 ± 0.10, and -1.80 ± 0.14, respectively (see Table I). The slope for the $C^{2+} + O^+ + O$ channel does not match with the theoretically predicted slope for sequential decay and this island is found to be of nearly dumbbell shape; thus a concerted dissociation should be the dominant process for this channel. For the $O^{2+} + C^+ + O$ channel, the shape of the island is a parallelogram with nearly vertical ends, suggesting s(i) to be the dominant process, even though the slope does not agree fully with the theoretically predicted slope for this process. For the $O^{2+} + O^+ + C$ channel, the slope of this island follows a sequential process, although it is difficult to distinguish between s(i) or s(d) processes by the observed value of the slope. The island is dumbbell shaped, thus the s(i) process should be operative in this case. In all the above cases, the KEs of individual ions are found to be almost equal for the O fragments, whereas it is found to be distributed close to zero for the C fragment as discussed in next paragraph. This suggests that in each of these cases, concerted processes may also make a significant, if not dominant, contribution. Similar observations were found in the earlier reported results of low-energy electron and photon impact dissociations of CO_2 [21,27,30].

The KER distributions derived for all of the incomplete fragmentation channels are shown in Fig. 3(c); the peak of KER distributions shifts to higher values as the degree of ionization of the CO_2 molecule is increased from two to three because of greater repulsion between the positive charges resulting in higher values of KER. The broad distributions of the KERs have a similar origin, as explained earlier in Sec. IV A. The estimated maximum released energy in these incomplete Coulomb fragmentation processes is *not* very accurate and hence the mean KER values are not derived for these cases but, rather, average values of the KEs of individual fragments are obtained (not shown). In the following discussion, the uncertainties in the average KEs are ± 0.3 eV for ionic fragments and about ± 0.9 eV for the undetected neutral fragments. For the $C^+ + O^+ + O$ dissociation channel of $CO_2{}^{2+}$, the average values of KEs of the three fragments are about 2.0, 7.0, and 6.4 eV, respectively. However, for the $O^+ + O^+ + C$ channel, the average KEs of the three fragments are found to be about 7.0, 6.6, and 2.5 eV, respectively; the faster O^+ ion is found to have an additional contribution in KE distribution very close to zero, which indicates that there are two distinct dissociation channels involving bent states as discussed above. For the dissociation of $CO_2{}^{3+}$ into $C^{2+} + O^+ + O$, $O^{2+} + C^+ + O$, and $O^{2+} + O^+ + C$, the KEs of carbon fragments are found to be distributed close to zero energy with average values $<$3.0 eV, whereas the oxygen fragments evolve with higher kinetic energies ($>$8.0 eV) irrespective of their final charge states (q), including $q = 0$, showing that the O fragments are emitted back to back, leaving the central C fragment at rest in most cases.

V. SUMMARY AND CONCLUSIONS

We have used a linear TOF spectrometer equipped with a multihit, position-sensitive detector to measure the momentum vectors of the fragment ions generated from 12-keV electron collisions with a CO_2 molecule. The angular and momentum correlations of these ions in their doubly and triply ionized parent precursor states are obtained which show the presence of bent molecular geometries of these states. By making use of a method devised by Eland [11,42] and experimentally observed KEs and angular distributions of fragments, the concerted and/or sequential nature of dissociation is suggested for different coincidence channels arising from the dissociation of CO_2^{2+} and CO_2^{3+}. The $C^+ + O^+ + O$, $O^{2+} + C^+ + O$, and $O^{2+} + O^+ + C$ channels are found to arise from concerted as well as s(i) processes, whereas the $O^+ + O^+ + C$, $C^{2+} + O^+ + O$, and $C^+ + O^+ + O^+$ channels arise from pure concerted processes. Furthermore, the KER distributions for these dissociation channels are also obtained. The CE model is found to overestimate our experimental KER values for the complete Coulomb fragmentation of CO_2^{2+} and CO_2^{3+} due to its oversimplified point-charge assumption.

ACKNOWLEDGMENTS

This work was supported by the Department of Science and Technology (DST), New Delhi, under the Research Project SR/S2/LOP-09/2006. The help received from Achim Czasch (RoentDek Handles) for the data analysis is gratefully acknowledged. P.B., R.S., and N.Y. thankfully acknowledge partial support from the Board of Research in Fusion Science & Technology (BRFST, Ahmedabad) and the Council of Scientific and Industrial Research (CSIR, New Delhi) during the progress of this work.

[1] D. Mathur, Phys. Rep. **391**, 1 (2004).
[2] S. D. Price, Phys. Chem. Chem. Phys. **5**, 1717 (2003).
[3] B. Boudaiffa, P. Cloutier, D. Hunting, M. A. Huels, and L. Sanche, Science **287**, 1658 (2000).
[4] U. Werner, K. Beckord, J. Becker, and H. O. Lutz, Phys. Rev. Lett. **74**, 1962 (1995).
[5] B. Siegmann, U. Werner, H. O. Lutz, and R. Mann, J. Phys. B **35**, 3755 (2002).
[6] B. Bapat and V. Sharma, J. Phys. B **40**, 13 (2007).
[7] H. Hasegawa, A. Hishikawa, and K. Yamanouchi, Chem. Phys. Lett. **349**, 57 (2001).
[8] N. Neumann, D. Hant, L. Ph. H. Schmidt, J. Titze, T. Jahnke, A. Czasch, M. S. Schöffler, K. Kreidi, O. Jagutzki, H. Schmidt-Böcking, and R. Dörner, Phys. Rev. Lett. **104**, 103201 (2010).
[9] W. C. Wiley and I. H. McLaren, Rev. Sci. Instrum. **26**, 1150 (1955).
[10] L. J. Frasinski, K. Codling, and P. A. Hatherly, Science **246**, 1029 (1989).
[11] J. H. D. Eland, Mol. Phys. **61**, 725 (1987).
[12] M. R. Bruce, L. Mi, C. R. Sporleder, and R. A. Bonham, J. Phys. B **27**, 5773 (1994).
[13] J. Ullrich, R. Dörner, and H. Schmidt-Böcking, Phys. News **1996**, 12 (1997).
[14] H. Schmidt-Böcking, V. Mergel, L. Schmidt, R. Dörner, O. Jagutzki, K. Ullmann, T. Weber, H. J. Lüdde, E. Weigold, and A. S. Kheifets, Radiat. Phys. Chem. **68**, 41 (2003).
[15] W. Eberhardt, E. W. Plummer, I.-W. Lyo, R. Carr, and W. K. Ford, Phys. Rev. Lett. **58**, 207 (1987).
[16] M. Neeb, M. Biermann, and W. Eberhardt, J. Electron Spectrosc. Relat. Phenom. **69**, 239 (1994).
[17] O. Witasse, O. Dutuit, J. Lilensten, R. Thissen, J. Zabka, C. Alcaraz, P.-L. Blelly, S. W. Bougher, S. Engel, L. H. Andersen, and K. Seiersen, Geophys. Res. Lett. **29**, 1263 (2002).
[18] L. Cao, G. Bala, K. Caldeira, R. Nemani, and G. Ban-Weiss, Proc. Natl. Acad. Sci. USA **107**, 9513 (2010).
[19] L. J. Frasinski, P. A. Hatherly, K. Codling, M. Larsson, A. Persson, and C.-G. Wahlström, J. Phys. B **27**, L109 (1994).
[20] T. Masuoka, E. Nakamura, and A. Hiraya, J. Chem. Phys. **104**, 6200 (1996).
[21] C. Tian and C. R. Vidal, Phys. Rev. A **58**, 3783 (1998).
[22] J. H. Sanderson, T. Nishide, H. Shiromaru, Y. Achiba, and N. Kobayashi, Phys. Rev. A **59**, 4817 (1999).
[23] L. Adoui, M. Tarisien, J. Rangama, P. Sobocinsky, A. Cassimi, J.-Y. Chesnel, F. Frémont, B. Gervais, A. Dubois, M. Krishnamurthy, S. Kumar, and D. Mathur, Phys. Scr., T **T92**, 89 (2001).
[24] N. Saito, Y. Maramatsu, H. Chiba, K. Ueda, K. Kubozuka, I. Koyano, K. Okada, O. Jagutzki, A. Czasch, T. Weber, M. Hattass, H. Schmidt-Böcking, R. Moshammer, M. Lavollée, and U. Becker, J. Electron Spectrosc. Relat. Phenom. **141**, 183 (2004).
[25] A. E. Slattery, T. A. Field, M. Ahmad, R. I. Hall, J. Lambourne, F. Penent, P. Lablanquie, and J. H. D. Eland, J. Chem. Phys. **122**, 084317 (2005).
[26] L. Adoui, T. Muranaka, M. Tarisien, S. Legendre, G. Laurent, A. Cassimi, J.-Y. Chesnel, X. Fléchard, F. Frémont, B. Gervais, E. Giglio, and D. Hennecart, Nucl. Instrum. Methods Phys. Res. B **245**, 94 (2006).
[27] R. K. Singh, G. S. Lodha, V. Sharma, I. A. Prajapati, K. P. Subramanian, and B. Bapat, Phys. Rev. A **74**, 022708 (2006).
[28] V. Sharma, B. Bapat, J. Mondal, M. Hochlaf, K. Giri, and N. Sathyamurthy, J. Phys. Chem. A **111**, 10205 (2007).
[29] J. P. Brichta, S. J. Walker, R. Helsten, and J. H. Sanderson, J. Phys. B **40**, 117 (2007).
[30] S. J. King and S. D. Price, Int. J. Mass Spectrom. **272**, 154 (2008).
[31] Z. D. Pešić, D. Rolles, R. C. Bilodeau, I. Dimitriu, and N. Berrah, Phys. Rev. A **78**, 051401(R) (2008).
[32] M. Alagia, P. Candori, S. Falcinelli, M. Lavollée, F. Pirani, R. Richter, S. Stranges, and F. Vecchiocattivi, J. Phys. Chem. A **113**, 14755 (2009).
[33] N. W. Winter, C. F. Bender, and W. A. Goddard, Chem. Phys. Lett. **20**, 489 (1973).
[34] H. Hogreve, J. Phys. B **28**, L263 (1995).
[35] M. Hochlaf, F. R. Bennett, G. Chambaud, and P. Rosmus, J. Phys. B **31**, 2163 (1998).
[36] T. A. Field and J. H. D. Eland, Chem. Phys. Lett. **303**, 144 (1999).

[37] B. Siegmann, U. Werner, and H. O. Lutz, Austr. J. Phys. **52**, 545 (1999).
[38] U. Brinkmann, A. Reinköster, B. Siegmann, U. Werner, H. O. Lutz, and R. Mann, Phys. Scr., T **T80**, 171 (1999).
[39] R. Singh, P. Bhatt, N. Yadav, and R. Shanker, Meas. Sci. Technol. **22**, 055901 (2011).
[40] P. Bhatt, R. Singh, N. Yadav, and R. Shanker, Phys. Rev. A **84**, 042701 (2011).
[41] RoentDek Handles GmbH [http://www.roentdek.com/].
[42] J. H. D. Eland, Laser Chem. **11**, 259 (1991).
[43] S. Hsieh and J. H. D. Eland, J. Chem. Phys. **103**, 1006 (1995).
[44] C. E. M. Strauss and P. L. Houston, J. Phys. Chem. **94**, 8751 (1990).
[45] Y. Itikawa, J. Phys. Chem. Ref. Data **31**, 749 (2002).